ESTIMATION OF INUNDATED AREAS DURING THE 2011 FLOODS IN THE CHAO PHRAYA RIVER BASIN USING SAR AND OPTICAL SATELLITE IMAGERY

Keisuke Kitamura[1], Tsuyoshi Kinouchi[2], Winai Liengcharernsit[3], and Atchara Komsai[4]

[1] Department of Environmental Science and Technology, Tokyo Institute of Technology, Kanagawa, Japan, Tel: (814) 59245515, e-mail: kitamura.k.ac@m.titech.ac.jp
[2] Department of Environmental Science and Technology, Tokyo Institute of Technology, Kanagawa, Japan, Tel: (814) 59245524, e-mail: kinouchi.t.ab@m.titech.ac.jp
[3] Faculty of Engineering, Kasetsart University, Bangkok, Thailand, e-mail: fengwnl@ku.ac.th
[4] Department of Environmental Science and Technology, Tokyo Institute of Technology, Kanagawa, Japan, Tel: (814) 59245515, e-mail: komsai.a.aa@m.titech.ac.jp

Received Date: March 31, 2014

Abstract

In 2011, massive flooding and inundation in the Chao Phraya River basin, in Thailand, caused serious damage to various activities for a prolonged period of time. Although snapshot images of the inundated area are available, detailed information including temporal changes of the inundated areas and the relationship with meteorological and hydrological conditions are not well documented, particularly for the middle and upper sections of the basin. Therefore, we conducted an analysis using two types of satellite data, HJ-1A and Envisat, to better understand behavior of the large-scale inundation occurred in 2011, focusing on the middle section of the Chao Phraya River basin. In the analysis, water surface in selected domains was extracted using the *NDWI* value calculated from HJ-1A data. The threshold value of the Envisat ASAR image was then adjusted so that the inundated area estimated from Envisat gives the closest possible match with that estimated from HJ-1A. Finally, the inundated area was estimated for the whole study domain based on the same threshold value from the Envisat data. Results indicated that the inundated area began to extend along the Yom and Nan rivers in early August and continued to spread down to the Nakhon Sawan city area until October. A significant increase in inundated areas occurred between September 2 and September 13, during which higher rainfall intensity was observed. Even after the water level in rivers receded below the bank-full elevation, large areas were left inundated along rivers, particularly over low-lying marsh and paddy fields. In addition, several areas located far from rivers were also inundated, which was likely a consequence of water ponding in paddy fields.

Keywords: Chao Phraya River basin, Estimation of inundated area, Flood in 2011, Satellite data

Introduction

In 2011, massive flooding occurred in the Chao Phraya River basin in Thailand due to an extremely large amount of rainfall over extensive areas [1], which was partly due to a series of major tropical cyclones and typhoons passing over the basin during the wet season. This caused large-scale inundations in many regions of the basin for a prolonged period and resulted in significant damages to various types of sectors.

For emergencies, satellite images help understand the extent and transition of inundated areas across a large domain. For example, UNOSAT estimated inundated areas

during the 2011 floods using multispectral optical data from the Moderate Resolution Imaging Spectrometer (MODIS) [2]. However, due to the limited number of snapshots with relatively coarse resolution (250 m), how the inundated area changed temporally and spatially during the massive 2011 floods remained unclear. Trigg et al. [3] analyzed inundation in the lower plains of the Chao Phraya River based on MODIS data. They focused on movement of flood water in greater Bangkok, while the upstream areas which feed into the lower Chao Phraya River were not well analyzed and documented. In view of the flood impact on agricultural production, MODIS data was used in combination with inundation area information generated by GISTDA, based on the satellite imaginary of RADARSAT 1 and 2, to quantify the flood-affected rice cultivation areas in the Chao Phraya River basin [4]. However, the information quality of the inundated area map from GISTDA was difficult to obtain. In addition, an analysis of flooded areas in conjunction with meteorological and hydrological conditions is rarely found. Therefore, this study attempts to attain more detailed information on the spatial extent and temporal change of inundated areas and the causal factors. We focused on the middle section of the Chao Phraya River basin above the Chao Phraya Dam and the Nakon Sawan City, since the area is considered to have a significant hydrological impact on downstream flooding in the lowland plains. For this purpose, we utilized two types of satellite data, multispectral optical band data from a Chinese satellite (HJ-1A) and C-band synthetic aperture radar (SAR) data from the Envisat satellite, together with meteorological, hydrological, and land use information covering the middle section of the Chao Phraya River basin.

In previous studies, different types of satellite data were utilized to detect inundated areas under various geographical and biological settings (e.g., inundation mapping for the Murray-Darling Basin, Australia using MODIS data and Landsat TM/ETM+ [5], real-time flood mapping of the Thailand Central plain using RADARSAT and MODIS data [6] and characterization of wetland inundation in the Florida Everglades using MODIS data [7]). Because of its high temporal resolution and wide spatial coverage, MODIS data is a popularly used source of optical band satellite images for the detection of land surface conditions, however, its usability is affected by cloud cover and its moderate resolution of 250 m is not fine enough to detect in detail the condition of inundated areas. Data from SAR, on the other hand, is not affected by the cloud cover, making it more suitable for estimating inundated areas in large domains [8] [9]. The SAR imagery obtained by RADARSAT and Envisat is solely used to determine the extent of the inundated areas [10] [11], often supported by visual interpretations based on clear elevation changes, lined structures (i.e., roads and embankments), and water level information at control points. Auynirundronkool et al. [6] applied both RADATSAT and MODIS for automated instant time flood detection in the Thailand Central plain, with MODIS data used to overview the entire area, while RADARSAT data was used to classify the flood areas. Hoque et al. [12] utilized RADARSAT data to separate out areas covered by water and compared the results with classified maps obtained from LANDSAT ETM+ data. However, no similar works were found to quantify the spatial and temporal characteristics of devastating inundation caused by the 2011 flood in the Chao Phraya River basin using both SAR and optical satellite imagery.

In this study, we employed SAR and optical satellite imagery to detect temporal changes of inundated areas in the middle section of the Chao Phraya River basin to better understand behavior of the large-scale inundation occurred in 2011. Optical data was used to delineate the boundary of inundated areas for selected cloud-free domains, which were further used to set a threshold value of back-scattering intensity for the SAR signal to define the inundation area in a larger domain. Consequently, the change in inundated areas using higher temporal resolution (150 m) was discussed with regard to the influential

factors of inundation in connection with the rainfall, the water level in rivers, and the land use of riverine areas.

Study Area

The Chao Phraya River basin (total area: 158×10^3 km^2) covers approximately one-third of Thailand's land area. We focused on the middle section of the basin, where the four tributary rivers, i.e., Ping, Wang, Yom, and Nan, flow down through flood plains and merge in the Nakhon Sawan city area (Figure 1, domain A) forming the origin of the Chao Phraya River. From this point, the Chao Phraya River flows southward to the Gulf of Thailand through the Ayutthaya city area and the Bangkok Metropolitan region, supplying water resources for agriculture, industry, and other urban activities, in addition to being used for transportation and flood control. Our study area is shown in Figure 1 (total area: 57×10^3 km^2), in which the target domains for determining the satellite data threshold values are indicated by the black solid boxes A–E with the size of 6 km × 6 km for domain A and 10 km × 10 km for others.

The climate of the study area is characterized by the tropical monsoon, for which the wet season is typically from May to October. According to the data obtained from the Thai Meteorological Department (TMD), the mean annual precipitation in the study area is approximately 1,300 mm, while annual precipitation in 2011 was 1,700 mm. Paddy fields and other agricultural fields are the dominant land use in the low lying areas, which are

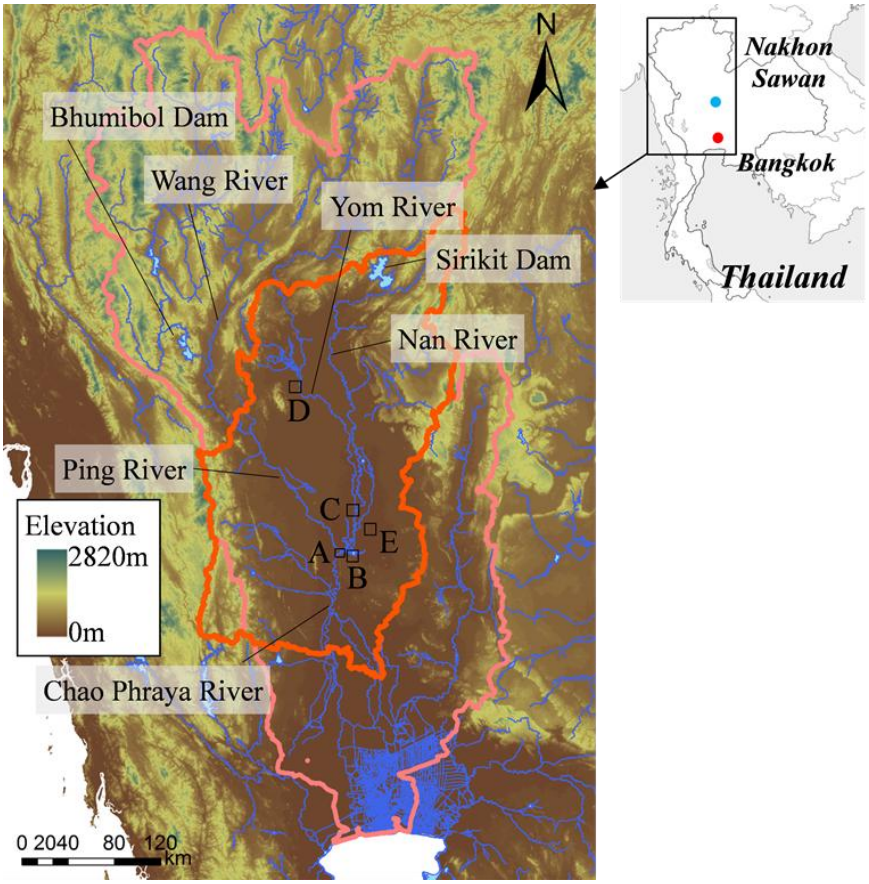

Figure 1. A map showing the study area (orange line), Chao Phraya River Basin (pink line), stream network, elevation, and domains (A–E) for determining satellite data threshold values

surrounded by mountain regions. The lower reaches of the four tributaries have very small bottom slopes ranging from 1/5000 to 1/10000, resulting in a limited discharge capacity and high potential for inundation along the river.

Methodology

Outline of Data Analysis

Data from two types of satellites, HJ-1A and Envisat, was utilized. HJ-1A is operated by China Centre for Resources Satellite Data and Application (CRESDA), with its data archived in the Satellite Center of Kasetsart University. The HJ-1A data used in this study has four visible bands (0.43–0.52 μm, 0.52–0.60 μm, 0.63–0.69 μm, and 0.76–0.90 μm) with a 30 m resolution. For Envisat, operated by the European Space Agency (ESA), the C-band data from the Advanced Synthetic Aperture Rader (ASAR) onboard was used in our analysis. The C-band ASAR image recorded in HH polarization mode was used with a ground resolution of approximately 150 m.

HJ-1A images can detect land cover conditions such as vegetation and soil, however, cannot be used when the sky is overcast, while ASAR detects surface conditions irrespective of cloud cover (Figure 2). The back-scattering intensity is known to decrease if the surface is covered by water, which enables identification of inundated areas. Thus, inundated areas were identified by following several steps which take advantage of each sensor's characteristics. Firstly, a specific domain under cloud-free condition was visually selected (domains A, C, D, and E in Figure 1) and the inundated areas extracted by introducing a Normalized Difference Water Index (*NDWI*) [13], which is calculated from raw digital numbers obtained from band 2 (0.52–0.60 μm) and band 4 (0.76–0.90 μm) HJ-1A outputs. The threshold value of *NDWI* for separating a water surface from other land surface conditions was determined enabling a reproduction of the inundated areas detectable from the visible image. This result was then utilized to set a threshold value for

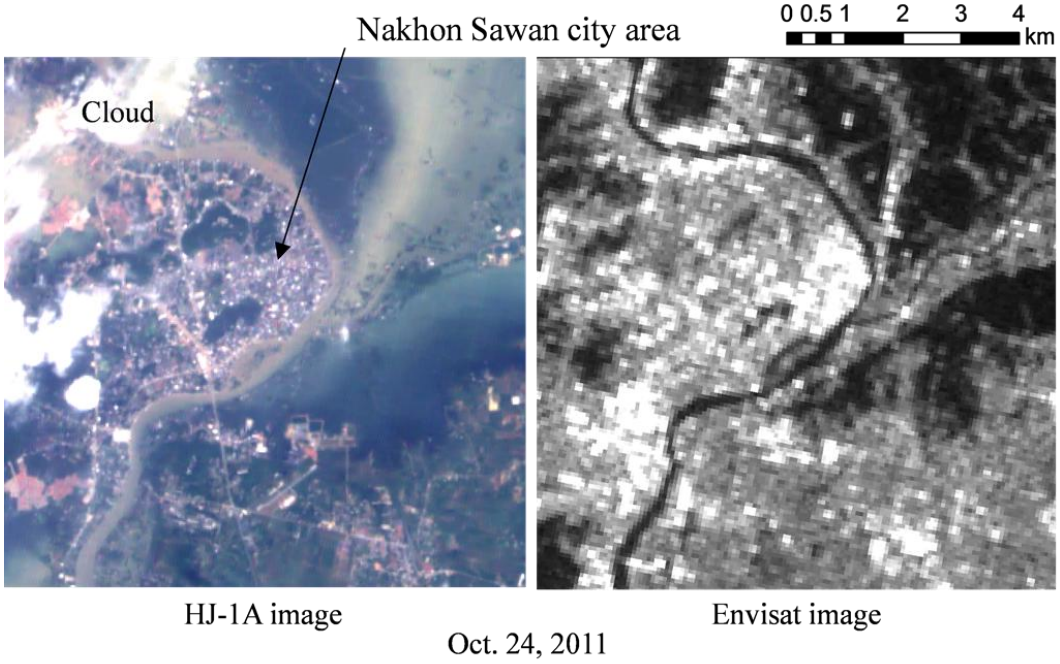

Figure 2. Visible image of HJ-1A (left) and Envisat's ASAR image (right) covering the test domain A

the ASAR signal back-scattering intensity, by comparing inundated areas obtained from HJ-1A and Envisat for a test domain (B–E). Finally, the threshold value for the back-scattering intensity was applied to the whole study area.

To discuss the physical factors affecting inundation, we collected hydrological and meteorological data, as well as the land use information. Data of daily rainfall and river water level in the study area were obtained from the Thai Meteorological Department (TMD) and Royal Irrigation Department (RID), respectively. Land use information was obtained from the Thai Land Development Department (LDD).

Selection of Threshold Values for *NDWI* and Back-Scattering Intensity

To extract the inundated areas in a given domain, *NDWI* was calculated from band 2 and band 4 of HJ-1A using Equation (1) [13].

$$NDWI = \frac{GREEN - NIR}{GREEN + NIR} \quad (1)$$

where *GREEN* and *NIR* are the surface reflectance in the visible (band 2) and near infrared (band 4), respectively. The *NDWI* value of the water surface varied due to factors such as the water turbidity and atmospheric conditions. Therefore, the threshold value of the *NDWI* for detecting water surface was set manually for each image taken on a different date to represent the borderline of visually detected inundated areas. The water surface of rivers was also obtained from the land-use map and the visible image. The river width at gaging stations located in each selected domain in the image, provided by RID, was also utilized to validate the threshold value.

Pixels of each ASAR image with a back-scattering intensity less than the threshold value were extracted as inundated areas. The threshold value of back-scattering intensity was determined for each ASAR image based on a measure (*CR*: Correspondence Ratio) defined by Equation (2) which provided the closest possible match between the inundated or non-inundated areas estimated from HJ-1A and Envisat for each test domain (B–E in Figure 1). The larger *CR* value means better matching of inundated and non-inundated areas estimated from HJ-1A and Envisat. Similar indices are found in Schumann et al. [14].

$$CR = \frac{a + d}{a + b + c + d} \quad (2)$$

where *a*, *b*, *c,* and *d* are the number of pixels satisfying the condition shown in the contingency table (Table 1).

Table 1. Contingency Table of Inundation

	Present in HJ-1A	**Absent in HJ-1A**
Present in Envisat	*a*	*b*
Absent in Envisat	*c*	*d*

Results and Discussion

Estimation of Inundated Areas in a Test Domain

Example results of inundated areas estimated from HJ-1A data are shown in Figure 4 for test domain A (Figure 3), which includes the area covering the confluence of the Ping and Nan rivers and the Beung Boraphet reservoir. Due to the overflow from the Ping and Nan

rivers, the inundated area on November 1 was larger than that on August 25. The overflow situation was confirmed by local residents during our field survey and from the water level monitored at the gaging station C.2 (Figure 3), which exceeded the left bank elevation for two

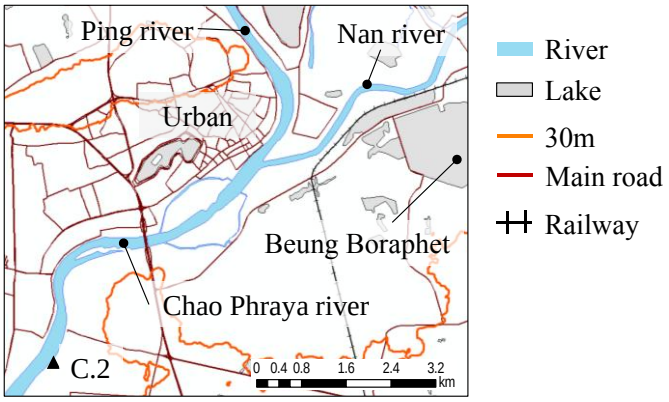

Figure 3. Domain A showing the confluence of the Ping and Nan Rivers, Beung Boraphet, the gaging station C.2 and contour lines

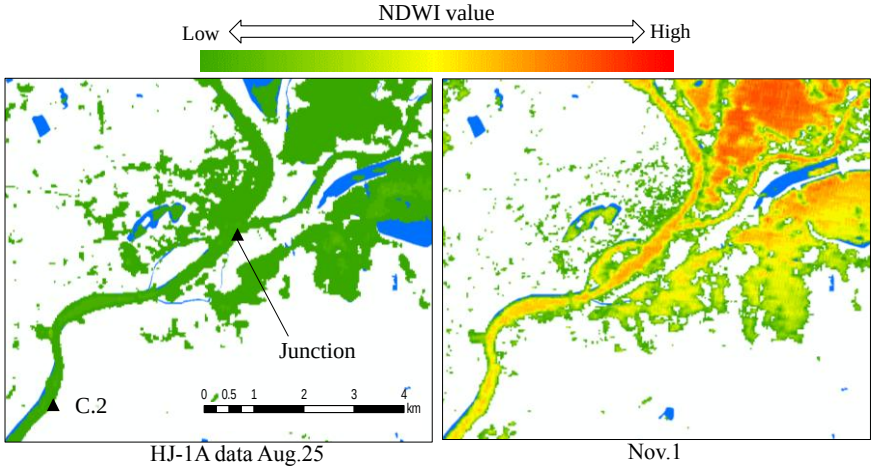

Figure 4. Inundated area in domain A estimated from HJ-1A data

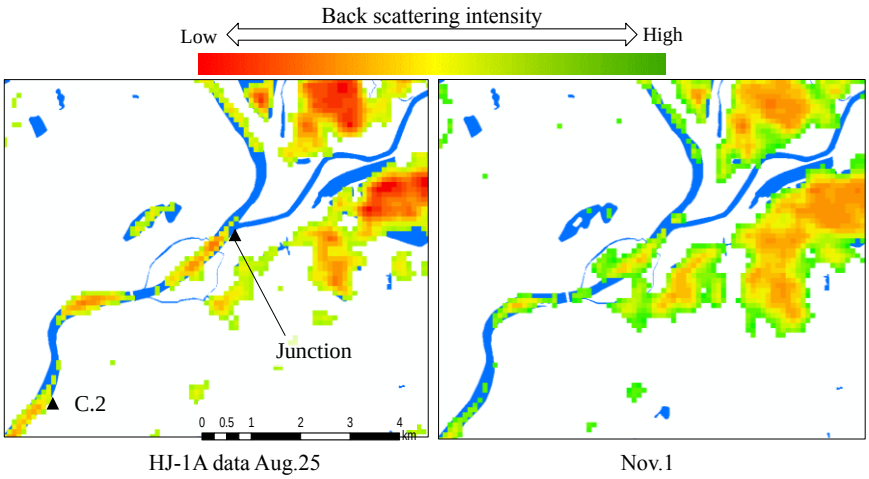

Figure 5. Inudated area in domain A estimated from Envisat's ASAR data

months, from early September to early November. Inundated areas estimated from Envisat's ASAR data for the same domain are shown in Figure 5. Unlike results from HJ-1A data, some urban areas and river surfaces are detected as non-inundated because of the coarser resolution of ASAR data.

Estimation of Inundated Regions in the Whole Study Area

Considering the limitation of HJ-1A due to the influence of cloud cover, inundated regions in the whole study area (Figure 1) were estimated from Envisat's ASAR data for ten periods (Figure 6), in which the threshold value of ASAR data calibrated for each period was applied. The value of *CR* calculated from Equation (2) ranged between 0.81 (December 1) and 0.98 (November 1), with the average for ten periods being 0.89. On August 3, the inundated areas were mostly located in the upper section of the Yom and Nan rivers. The inundated water then gradually spread over a wider area along the Yom and Nan rivers down to a region which included Nakhon Sawan City and Beung Boraphet by September 2 (Figure 6(b)–(d)). Between September 2 and September 13, the inundated area expanded significantly, paricularly in areas located to the east of Beung Boraphet, in the northern region confined by the Yom and Nan rivers, and the area bounded by the Ping and Yom rivers (Figure 6(e)). These areas showed a decreasing trend between September 13 and October 21, while the inundated areas closer to the confluence of the Ping and Nan rivers expanded over the same period. This was most likely due to the concentrated runoff from upstream areas and the flood water overflown from the Yom River to paddy fields and marsh lands. Between October 21 and November 12, the inundated regionsdid not change greatly, probably because there were fewer overflows due to a

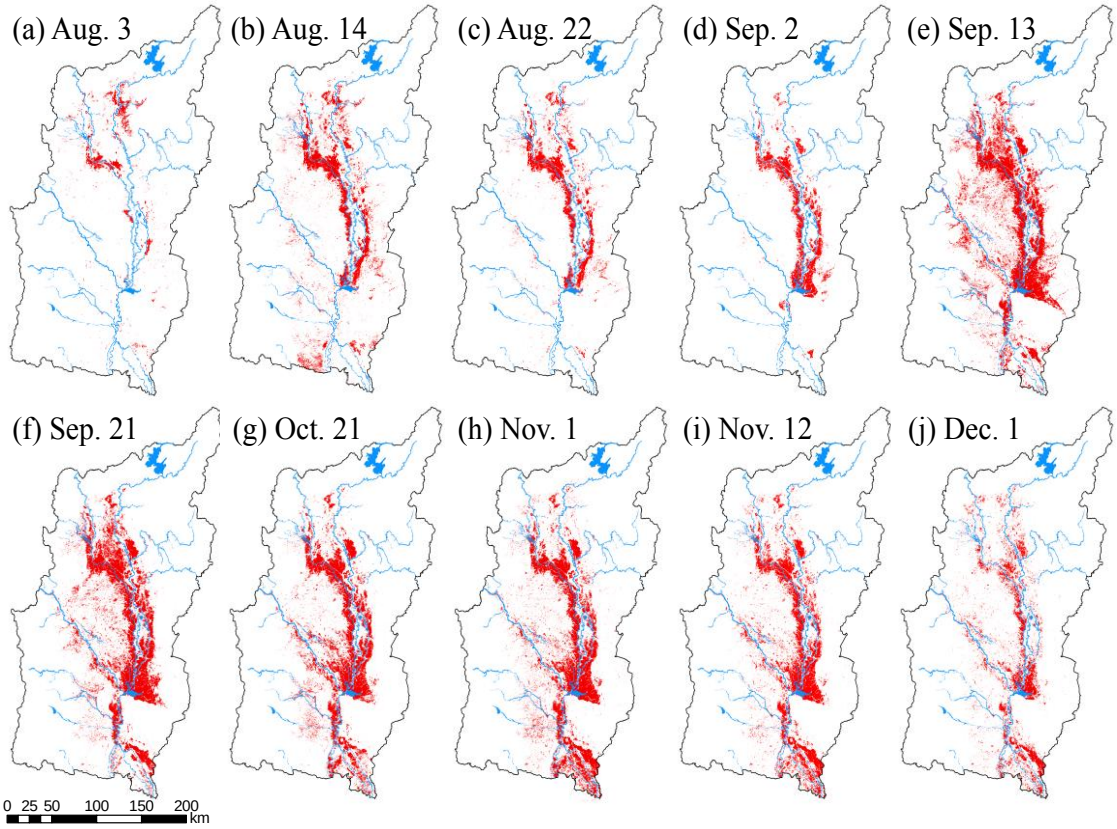

Figure 6. Inundated area in the study area estimated from Envisat's ASAR data for ten periods

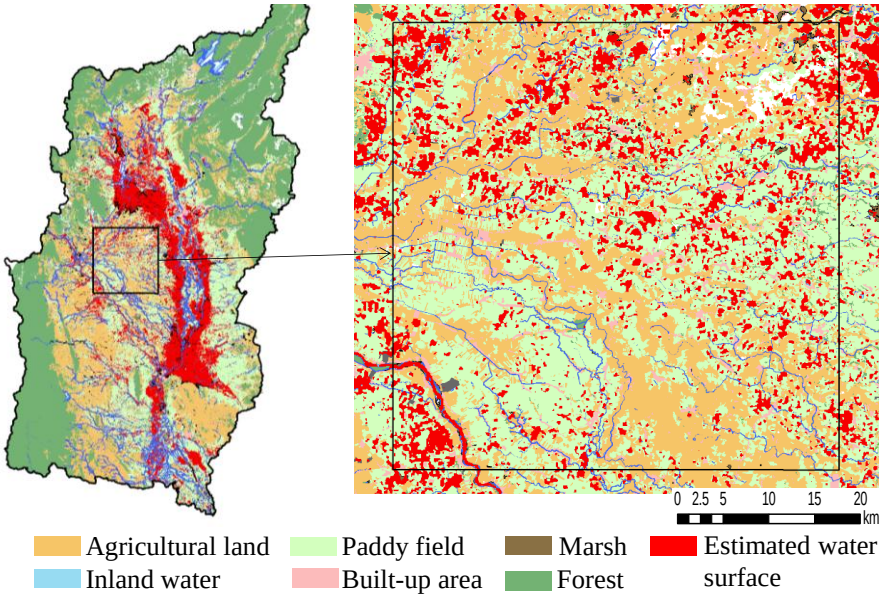

Figure 7. Overlaid map of land use and the inundated area estimated from Envisat's ASAR data on September 13

larger inundated water depth along the rivers. On December 1, an area along the Yom River (western side) and downstream along the Nan River (eastern side) was still inundated, although the water levels in the river were already lower than the bank-full elevation, which is shown later. This is attributed to a decreased ability to drain inundated waters from low-lying marsh lands and paddy fields. In addition, the Nakhon Sawan city area remained inundated due to a low ground elevation (Figure 3).

Land use data indicated that most of the water surface detected in the areas bounded by the Ping and Yom rivers on September 13 was distributed over areas classified as paddy fields (Figure 7). Normally, the second cropping season starts from July, when farmers may introduce waters to their paddy fields since most farmlands are rain fed. Even so, the water surface in the paddy fields is not detected before September 13. This result suggests that the detected water surface is likely due to the water ponding in paddy fields by the rainfall and surface runoff, which might have retarded the runoff to downstream areas. A large area along the Chao Phraya River between C.2 and the downstream end of the study area was found to be inundated between Sep. 13 and December 1, most likely because the river discharge exceeded the bank-full discharge capacity at the downstream reach of the Chao Phraya River, with the dike break and the collapse of the gate occurring during this period [15]. The inundation in this area would have been more serious if the larger discharge capacity of upstream rivers had been achieved to prevent local inundation.

Inundation Related to Meteorological and Hydrological Conditions

Accumulated rainfall at selected gauging stations (Figure 8(a)) is shown in Figure 8(b). Due to the Nock Ten typhoon which approached from the South China Sea in late July, a huge amount of rainfall was observed over the northern part of Chao Phraya River basin. This event was likely the main cause of the inundation detected along the upper section of Nan River on August 3 (Figure 6(a)). Other tropical storms and typhoons such as Haitang, Nesat, and Nalgae approached to the Indochina Peninsula during the late September and early October delivering a certain amount of rainfall, however, it seems that the impact of these events was limited as the inundated areas shrunk between September 21 and October 21 (Figure 6(f) and 6(g)).

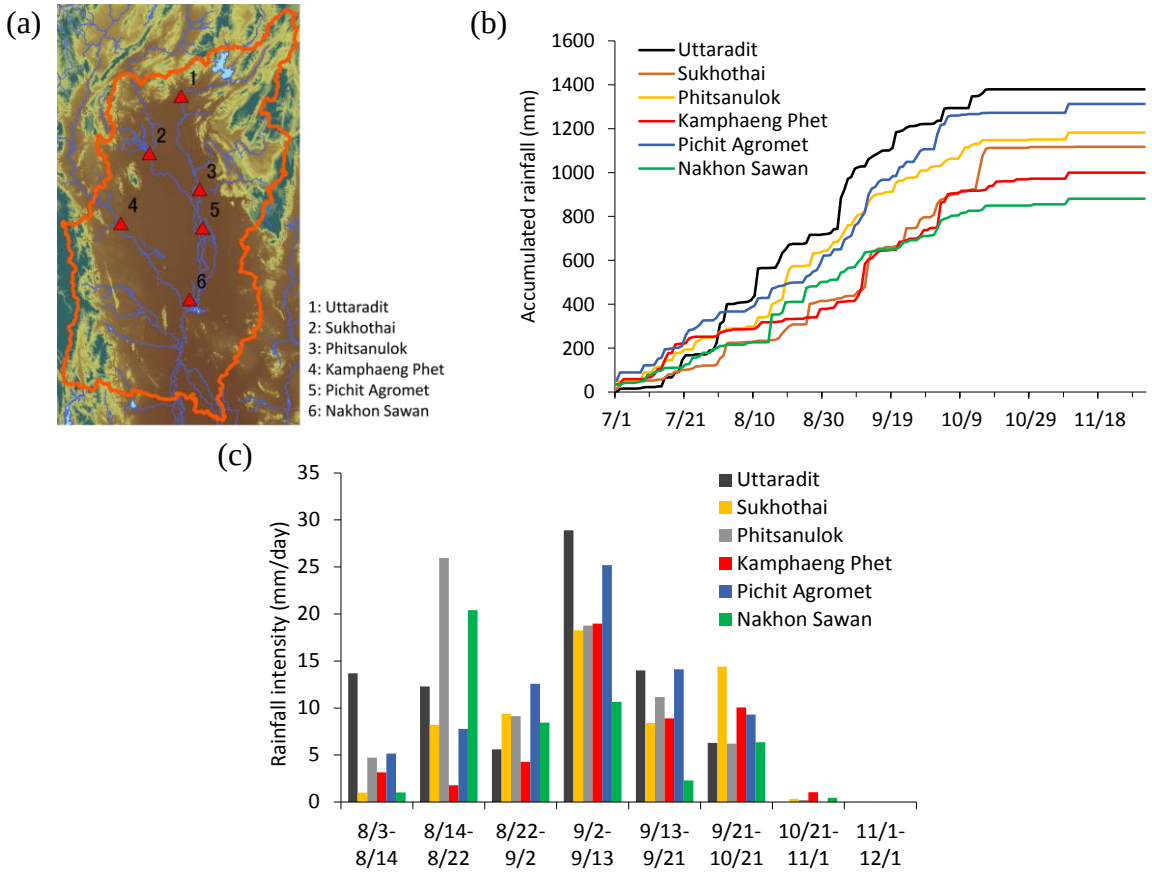

Figure 8. Rainfall gauge stations (a), accumulated rainfall (b) and rainfall intensity (c)

Figure 8(c) illustrates the relatively high rainfall intensity observed at each station between September 2 and September 13, which attributed to the overall expansion of inundated areas during this period, including local ponding over the area bounded by the Ping and Yom rivers (Figure 6(e) and Figure 7).

The temporal variation of water level at several gauging stations in the Yom and Nan rivers are shown in Figure 9, along with the change in inundated areas. At Y.16, the water level exceeded the bank-full elevation of the left side from July 14 to November 17. Although the water level was slightly lower than the bank-full elevation on the right side, the flattened variation of water level suggests that overflow likely occurred at some locations where the bank-full elevation is relatively low. A similar situation was observed for downstream locations such as Y.5. Along the Nan River, the bank-full flow condition was met at N.8A and N.67 from the middle of August to late October (N.8A) and early November (N.67), which is shorter than the period of bank-full flow condition along the Yom River (Y.16). As mentioned earlier, an inundated area was still detected even after the late October, when the water level receded below the bank-full elevation. The shorter duration of high water level in the Nan River is likely a consequence of regulated flood release from the upstream dam (Sirikit Dam) and the relatively large bank-full discharge capacity of the Nan River. Since October 21, the inundated area appears to have shrunk faster along the Nan River than the Yom River (Figure 9), which was attributed to the shorter duration of high water level in the former.

Conclusions

We analyzed two types of satellite data, HJ-1A and Envisat, to detect temporal changes of

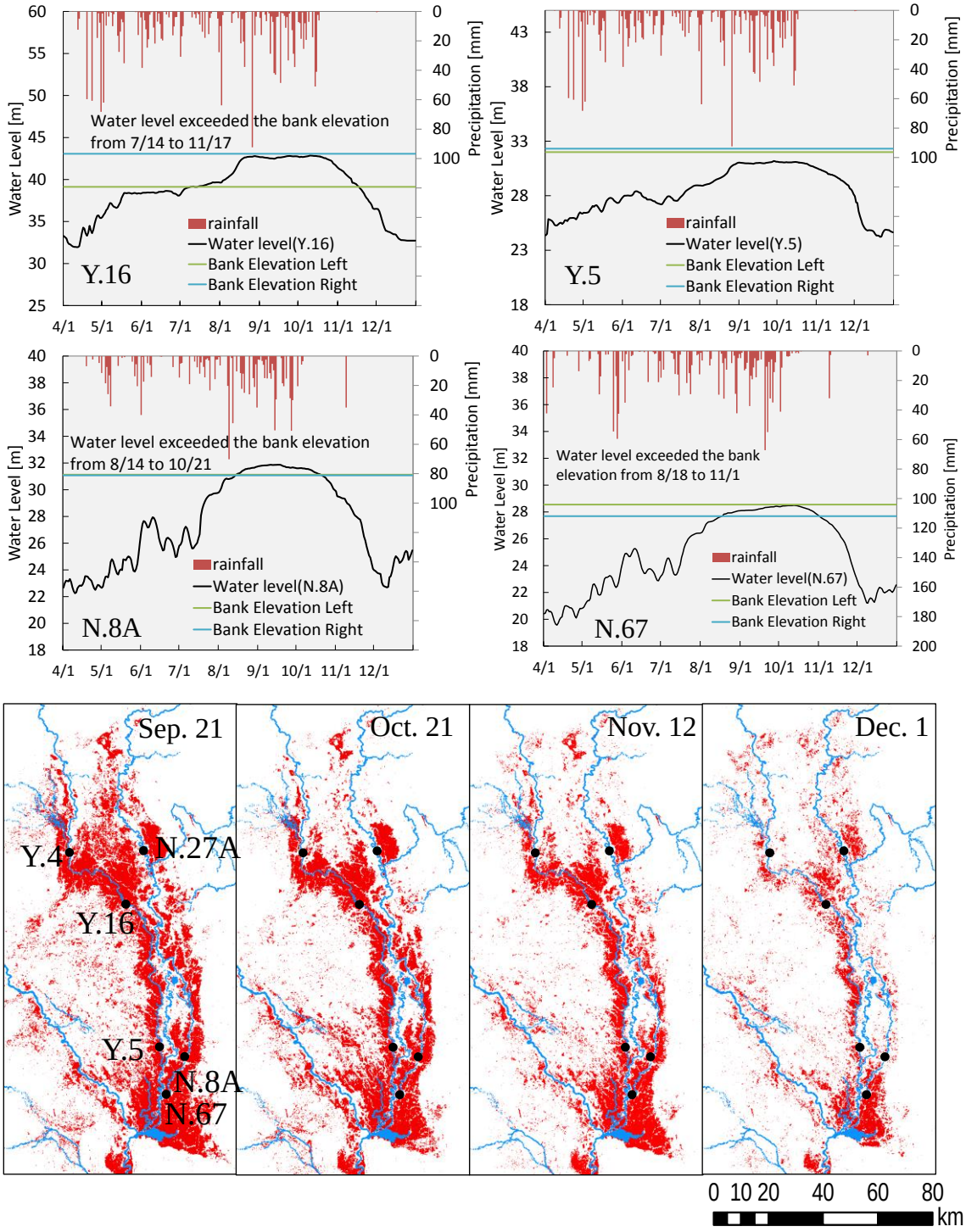

Figure 9. Variations of water level in the Yom and Nan rivers, location of gaging stations, and close-up views of areas inundated since September 21

inundated areas in the middle section of the Chao Phraya River basin to better understand behavior of the large-scale inundation that occurred in 2011. By introducing a threshold method to both HJ-1A and Envisat's ASAR data, the inundated area in the whole study domain was estimated for ten periods from August 3 to December 1. Results indicated that the inundated areas began to extend along the Yom and Nan rivers in early August and continued to spread down to the Nakhon Sawan city area until October, mainly due to river

overflow. Even after the water level in rivers receded below the bank-full elevation, large areas were left inundated for a long period, particularly over the low-lying marsh and paddy fields along the Yom and Nan rivers. Between September 2 and September 13, when high rainfall intensity was observed over the study domain, large plains between the Ping and Yom rivers were detected as being inundated. This localized inundation was likely due to water ponding in paddy fields, which might have relieved the inundation in downstream areas. A further study is necessary to understand the hydrological effects on the downstream areas due to the inundation in the middle section of the Chao Phraya River basin.

Because Envisat ended its operation in 2012, the methodology employed in this study cannot be directly applied for estimating inundated areas in other regions thereafter. However, the advantage of high spatial and temporal resolutions of HJ-1A and the use of SAR satellites such as ALOS and RADARSAT will ensure the detection of large-scale inundation in regions located under similar climatic and geographic conditions.

Acknowledgments

This research was funded by the Asian Core Program of Japan Society for the Promotion of Science (JSPS), National Research Council of Thailand (NRCT), and Engineering Research and Development for Technology (ERDT). We are grateful for the satellite data of HJ-1A and Envisat provided by Kasetsart University and ESA, respectively, hydrological and meteorological data provided by RID and TMD, respectively, and land use data provided by LDD.

References

[1] E.L. Gale, and M.A. Saunders, "The 2011 Thailand flood: Climate causes and return periods," *Weather*, Vol. 68, pp. 233–237, 2013.

[2] UNITAR/UNOSAT, *Overview of Flood Waters over Central Provinces, Thailand*, Product ID: 1600 - English, GLIDE: FL-2011-000135-THA, NASA Rapid Response, Geneva, Switzerland: UNITAR, October 11, 2011.

[3] M.A. Trigg, K. Michaelides, J.C. Neal, and P.D. Bates, "Surface water connectivity dynamics of a large scale extreme flood," *Journal of Hydrology*, Vol. 505, pp. 138-149, 2013.

[4] N.T. Son, C.F. Chen, C.R. Chen, and L.Y. Chang, "Satellite-based investigation of flood-affected rice cultivation areas in Chao Phraya river delta, Thailand," *ISPRS Journal of Photogrammetry and Remote Sensing*, Vol. 86, pp. 77-88, 2013.

[5] C. Huang, Y. Chen, and J. Wu, "Mapping spatio-temporal flood inundation dynamics at large river basin scale using time-series flow data and MODIS imagery," *International Journal of Applied Earth Observation and Geoinformation*, Vol. 26, pp. 350–362, 2014.

[6] K. Auynirundronkoola, N. Chen, C. Peng, C. Yang, J. Gong, and C. Silapathong, "Flood detection and mapping of the Thailand central plain using RADARSAT and MODIS under a sensor web environment," *International Journal of Applied Earth Observation and Geoinformation*, Vol. 14, pp. 245-255, 2012.

[7] C. Ordoyne, and M.A. Friedl, "Using MODIS data to characterize seasonal inundation patterns in the Florida everglades," *Remote Sensing of Environment*, Vol. 112, pp. 4107-4119, 2008.

[8] G. Schumann, P.D. Bates, M.S. Horritt, P. Matgen, and F. Pappenberger, "Progress in integration of remote sensing-derived flood extent and stage data and hydraulic models," *Reviews of Geophysics*, Vol. 47, RG4001, 2009.

[9] J.B. Henry, P. Chastanet, K. Fellah, and Y.L. Desnos, "Envisat multi-polarized ASAR

data for flood mapping," *International Journal of Remote Sensing*, Vol. 27, No. 10, pp. 1921-1929, 2006.

[10] A. Tarpanelli, L. Brocca, F. Melone, and T. Moramarco, "Hydraulic modelling calibration in small rivers by using coarse resolution synthetic aperture radar imagery," *Hydrological Processes*, Vol. 27, pp. 1321-1330, 2013.

[11] P. Matgen, G. Schumann, J.B. Henry, L. Hoffmann, and L. Pfister, "Integration of SAR-derived river inundation areas, high-precision topographic data and a river flow model toward near real-time flood management," *International Journal of Applied Earth Observation and Geoinformation*, Vol. 9, pp. 247-263, 2007.

[12] R. Hoque, D. Nakayama, H. Matsuyama, and J. Matsumoto, "Flood monitoring, mapping and assessing capabilities using RADARSAT remote sensing, GIS and ground data for Bangladesh," *Natural Hazards*, Vol. 57, pp. 525-548, 2011.

[13] S.K. McFeeters, "The use of the Normalized Difference Water Index (NDWI) in the delineation of open water features," *International Journal of Remote Sensing*, Vol. 17, No. 7, pp. 1425-1432, 1996.

[14] G. Schumann, P.D. Bates, M.S. Horritt, P. Matgen, and P. Pappenberger, "Progress in integration of remote sensing–derived flood extent and stage data and hydraulic models," *Reviews of Geophysics*, Vol. 47, RG4001, 2009.

[15] D. Komori, S. Nakamura, M. Kiguchi, A. Nishijima, D. Yamazaki, S. Suzuki, A. Kawasaki, K. Oki, and T. Oki, "Characteristics of the 2011 Chao Phraya River flood in Central Thailand," *Hydrological Research Letters*, Vol.6, pp. 41-46, 2012.